



Analysis and control of a dynamic model involving hypothalamic-pituitary-adrenal (HPA) axis

Lakshmi. N. Sridhar

Chemical Engineering Department, University of Puerto Rico, Mayaguez, PR 00681

Corresponding Author: Lakshmi. N. Sridhar, Chemical Engineering Department, University of Puerto Rico, Mayaguez, PR 00681

Received: April 20, 2025; **Published:** April 28, 2025

Abstract

The hypothalamic-pituitary-adrenal (HPA) axis links the nervous and endocrine systems' functions, which is of vital importance for maintaining homeostasis in mammalian organisms both under normal conditions and during stress. The integration of the nervous and endocrine systems' functions is very nonlinear and exhibits oscillatory behavior. Bifurcation analysis is a powerful mathematical tool used to deal with the nonlinear dynamics of any process. Several factors must be considered, and multiple objectives must be met simultaneously. Bifurcation analysis and multiobjective nonlinear model predictive control (MNL MPC) calculations are performed on a model of the hypothalamic-pituitary-adrenal (HPA) axis. The MATLAB program MATCONT was used to perform the bifurcation analysis. The MNL MPC calculations were performed using the optimization language PYOMO in conjunction with the state-of-the-art global optimization solvers IPOPT and BARON. The bifurcation analysis Hopf bifurcation points that lead to limit cycles. These Hopf points were eliminated using an activation factor that involves the tanh function. The multiobjective nonlinear model predictive control calculations converge to the Utopia point, which is the best solution.

Keywords: Bifurcation, optimization, control, hypothalamic-pituitary-adrenal (HPA) axis, Hopf

Introduction

Tsigos et al (2002)[1] investigated neuroendocrine factors and stress factors in Hypothalamic-pituitary-adrenal axis problems. Savic and Jelic (2005)[2] performed a theoretical study of hypothalamo-pituitary adrenocortical axis dynamics. Jelic et al (2005)[3] mathematically modelled the hypothalamic-pituitary-adrenal system activity. Lenbury et al (2005)[4] developed a delay-differential equation model of the feedback-controlled hypothalamus-pituitary-adrenal axis in humans. Kyrilov et al (2005)[5] modelled the oscillatory behavior of the hypothalamic-pituitary-adrenal axis. Savic et al (2006)[6] discussed the stability of a general delay differential model of the hypothalamo-pituitary-adrenocortical system. Smith et al (2006)[7] studied the role of the hypothalamic-pituitary-adrenal axis in neuroendocrine responses to stress. Gupta et al (2007)[8] showed that the inclusion of the glucocorticoid receptor in a hypothalamic pituitary adrenal axis model reveals bistability. Bairagi et al (2008)[9] discussed the variability in the secretion of corticotropin-releasing hormone, adrenocorticotrophic hormone and cortisol and understandability of the hypothalamic-pituitary-adrenal axis dynamics. Vinther et al(2011)[10] developed a minimal model of the hypothalamic-pituitary-adrenal axis. Jelic et al (2011)[11] discussed the predictive modeling of the hypothalamic-

pituitary-adrenal (HPA) function. Markovic et al (2011)[12], performed predictive modeling studies of the hypothalamic-pituitary-adrenal (HPA) axis response to acute and chronic stress. Markovic et al (2011)[13] investigated the, the stability of the extended model of the hypothalamic-pituitary-adrenal axis examined by stoichiometric network analysis. Andersen et al (2013)[14] performed mathematical modeling studies of the hypothalamic-pituitary-adrenal gland (HPA) axis, including hippocampal mechanisms. Postnova et al (2013)[15] developed a minimal physiologically based model of the HPA axis under influence of the sleep-wake cycles. Gudmand-Hoeyer et al (2014)[16] performed a Patient-specific modeling of the neuroendocrine HPA-axis and studied its relation to depression. Hosseinichimeh et al (2015)[17] performed additional modeling the hypothalamus-pituitary-adrenal axis. Malek et al (2015)[18] discussed the dynamics of the HPA axis and inflammatory cytokines. Markovic et al (2016)[19] investigated the cholesterol effects on the dynamics of the hypothalamic-pituitary-adrenal (HPA) axis. Cupic et al (2016)[20] studied the dynamic transitions in a model of the hypothalamic-pituitary-adrenal axis. Pierre et al (2016)[21] investigated the role of the hypothalamic-pituitary-adrenal axis in modulating seasonal changes in immunity. Abulseoud et al (2017)[22] demonstrated the existence of corticosterone oscillations during mania induction in the lateral hypothalamic kindled rat-Experimental observations. Stanojevic

et al (2017)[23] performed kinetic modelling of testosterone-related differences in the hypothalamic–pituitary–adrenal axis response to stress. Bangsgaard et al (2017)[24] performed patient-specific modelling studies of the HPA axis related to the clinical diagnosis of depression. Kim et al (2017)[25] performed mathematical modeling to improve diagnosis of post-traumatic and related stress disorders by perturbing the hypothalamic–pituitary–adrenal stress response system. Stanojevic et al (2017)[26] modelled the hypothalamic–pituitary–adrenal axis perturbations by externally induced cholesterol pulses of finite duration and with asymmetrically distributed concentration profiles. Kim LU et al (2017)[27] perturbed the hypothalamic pituitary–adrenal axis and developed a mathematical model for interpreting PTSD assessment tests. *Comput Psychiatry* 2017, 2:28-49. Kaslik et al (2018)[28] discussed the stability and demonstrated the existence of Hopf bifurcations for the hypothalamic–pituitary–adrenal axis model with memory. The aim of this paper is to 1) perform bifurcation studies on the hypothalamic–pituitary–adrenal axis model described in Cupic et al (2016)[20], demonstrate the existence of Hopf bifurcations and provide a strategy to eliminate them and 2) to perform multiobjective nonlinear model predictive control calculations on the same hypothalamic–pituitary–adrenal axis model. This document is organized as follows. The model equations for the hypothalamic–pituitary–adrenal axis model Cupic et al (2016)[20] is first described. This is followed by a description of the numerical methods (bifurcation analysis and MNLMPC). The results and discussion are then presented, followed by the conclusions.

Model Equations Cupic et al (2016)[20]

The model equations are

$$\begin{aligned} \frac{dx_1}{dt} &= (v_1 - (v_5 + v_6) - v_9) \\ \frac{dx_2}{dt} &= (v_2 - (v_4 + v_{10})) \\ \frac{dx_3}{dt} &= (v_4 - (v_5 + v_6) - v_7 - v_{11}) \\ \frac{dx_4}{dt} &= (v_5 + v_7 - v_8 - v_{12}) \\ \frac{dx_5}{dt} &= (v_3 + v_6 - v_8 - v_{13}) \end{aligned} \quad (1)$$

Where

$$\begin{aligned} v_1 &= k_1; v_2 = k_2; v_3 = k_3; v_4 = k_4 x_2; v_5 = k_5 x_1 x_3; v_6 = k_6 x_1 x_3; \\ v_7 &= k_7 x_3 (x_4^2); v_8 = k_8 x_5 (x_4^2); v_9 = k_9 x_1; \\ v_{10} &= k_{10} x_2; v_{11} = k_{11} x_3; v_{12} = k_{12} x_4; v_{13} = k_{13} x_5; \end{aligned}$$

The base parameters are

$$\begin{aligned} k_1 &= 1.38e-04; k_2 = 1.83e-08; k_3 = 6.09e-11; k_4 = 1.83e+04; k_5 = 11.94; k_6 = 9.552e-02; \\ k_7 &= 1.26e+14; k_8 = 7.05e+12; k_9 = 4.5e-02; k_{10} = 1.1e-01; k_{11} = 5.35e-02; k_{12} = 4.1e-01; \\ k_{13} &= 1.35e-01; \end{aligned}$$

(x_1, x_2, x_3, x_4) represent cholesterol, CRH, ACTH, cortisol, and aldosterone.

Bifurcation analysis

The MATLAB software MATCONT is used to perform the bifurcation calculations. Bifurcation analysis deals with multiple steady-states and limit cycles. Multiple steady states occur because of the existence of branch and limit points. Hopf bifurcation points cause limit cycles. A commonly used MATLAB program that locates limit points, branch points, and Hopf bifurcation points is MATCONT (Dhooge Govearts, and Kuznetsov, 2003[29]; Dhooge Govearts, Kuznetsov, Mestrom and Riet, 2004[30]). This program detects Limit points(LP), branch points(BP), and Hopf bifurcation points(H) for an ODE system

$$\frac{dx}{dt} = f(x, \alpha) \quad (3)$$

$x \in R^n$ Let the bifurcation parameter be α Since the gradient is orthogonal to the tangent vector,

The tangent plane at any point $w = [w_1, w_2, w_3, w_4, \dots, w_{n+1}]$ must satisfy

$$Aw = 0 \quad (4)$$

Where A is

$$A = [\partial f / \partial x \quad | \quad \partial f / \partial \alpha] \quad (5)$$

where $\partial f / \partial x$ is the Jacobian matrix. For both limit and branch points, the matrix $[\partial f / \partial x]$ must be singular. The $n+1$ th component of the tangent vector $w_{n+1} = 0$ for a limit point (LP) and for a branch point (BP) the matrix $\begin{bmatrix} A \\ w^T \end{bmatrix}$ must be singular. At a Hopf bifurcation point,

$$\det(2f_x(x, \alpha) @ I_n) = 0 \quad (6)$$

@ indicates the bialternate product while I_n is the n -square identity matrix. Hopf bifurcations cause limit cycles and should be eliminated because limit cycles make optimization and control tasks very difficult. More details can be found in Kuznetsov (1998[31]; 2009[32]) and Govaerts [2000] [33]

Hopf bifurcations cause unwanted oscillatory behavior and limit cycles. The tanh activation function (where a control value u is replaced by $(u \tanh u / \varepsilon)$) is commonly used in neural nets (Dubey et al 2022[34]; Kamalov et al, 2021[35] and Szandala, 2020[36]) and optimal control problems (Sridhar 2023[37]) to eliminate spikes in the optimal control profile. Hopf bifurcation points cause oscillatory behavior. Oscillations are similar to spikes, and the results in Sridhar(2024)[37] demonstrate that the tanh factor also eliminates the Hopf bifurcation by preventing the occurrence of oscillations. Sridhar (2024)[38] explained with several examples how the activation factor involving the tanh function successfully eliminates the limit cycle causing Hopf bifurcation points. This was because the tanh function increases the time period of the oscillatory behavior, which occurs in the form of a limit cycle caused by Hopf bifurcations.

Multiobjective Nonlinear Model Predictive Control (MNLMPC)

Flores Tlacuahuaz et al (2012)[39] developed a multiobjective nonlinear model predictive control (MNLMPC) method that is rigorous and does not involve weighting functions or additional constraints. This procedure is used for performing the MNLMPC calculations Here $\sum_{j=1}^n q_j(t_i)$ ($j=1,2,\dots,n$) represents the variables that need to be minimized/maximized simultaneously for a problem involving a set of ODE

$$\frac{dx}{dt} = F(x, u) \quad (7)$$

t_f being the final time value, and n the total number of objective variables and u the control parameter. This MNLMPC procedure first solves the single objective optimal control problem independently optimizing each of the variables $\sum_{j=1}^n q_j(t_i)$ individually. The minimization/maximization of $\sum_{j=1}^n q_j(t_i)$ will lead to the values q_j^* . Then the optimization problem that will be solved is

$$\min \left(\sum_{j=1}^n \sum_{t_i=0}^{t_i=t_f} (q_j(t_i) - q_j^*)^2 \right) \quad (8)$$

$$\text{subject to } \frac{dx}{dt} = F(x, u);$$

This will provide the values of u at various times. The first obtained control value of u is implemented and the rest are discarded. This procedure is repeated until the implemented and the first obtained control values are the same or if the Utopia point where $(\sum_{t=0}^{t_f} q_j(t_i) = q_j^*)$ for all j is obtained. Pyomo (Hart et al, 2017)[40] is used for these calculations. Here, the differential equations are converted to a Nonlinear Program (NLP) using the orthogonal collocation method. The NLP is solved using IPOPT (Wächter And Biegler, 2006)[41] and confirmed as a global solution with BARON (Tawarmalani, M. and N. V. Sahinidis 2005)[42].

The steps of the algorithm are as follows

Optimize $\sum_{t=0}^{t_f} q_j(t_i)$ and obtain q_j^* at various time intervals t_i . The subscript i is the index for each time step.

Minimize $(\sum_{j=1}^n (\sum_{t=0}^{t_f} q_j(t_i) - q_j^*))^2$ and get the control values for various times.

Implement the first obtained control values

Repeat steps 1 to 3 until there is an insignificant difference between the implemented and the first obtained value of the control variables or if the Utopia point is achieved. The Utopia point is when $\sum_{t=0}^{t_f} q_j(t_i) = q_j^*$ for all j .

Results and Discussion

When the bifurcation analysis was performed with k_4 as the bifurcation parameter, a Hopf bifurcation point was located at $(x_1, x_2, x_3, x_4, k_4)$ values of $(0.003067, 0, 0, 0, 0, 0.815058)$ as shown in curve AB in Fig. 1. When k_4 was modified to $k_4 \tanh(k_4)/100$ the Hopf bifurcation disappears. This is shown in curve AC in Fig. 1. When the bifurcation analysis was performed with k_5 as the bifurcation parameter, a Hopf bifurcation point was located at $(x_1, x_2, x_3, x_4, k_5)$ values of $(0.003067, 0, 0, 0, 0, 12.539816)$ as shown in curve AB in Fig. 2. When k_5 was modified to $k_5 \tanh(k_5)/100$ the Hopf bifurcation disappears. This is shown in curve AC in Fig. 2. When k_6 was the bifurcation parameter, a Hopf bifurcation point was located at $(x_1, x_2, x_3, x_4, k_6)$ values of $(0.003067, 0, 0, 0, 0, 2.869237)$ as shown in curve ABC in Fig. 3. When k_6 was modified to $k_6 \tanh(k_6)/100$ the Hopf bifurcation disappears. This is shown in the curve ABD in Fig. 3.

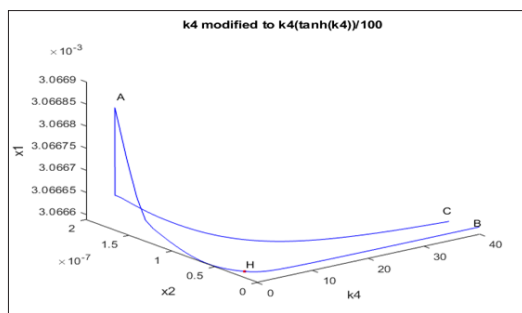


Figure 1: Bifurcation analysis with k_4 as bifurcation parameter.

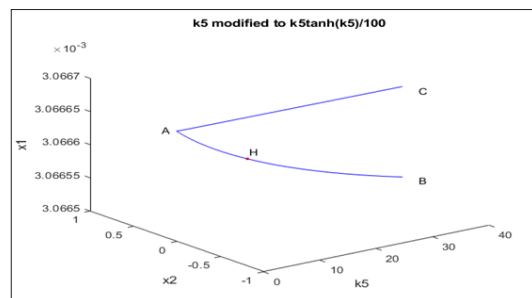


Figure 2: Bifurcation analysis with k_5 as bifurcation parameter.

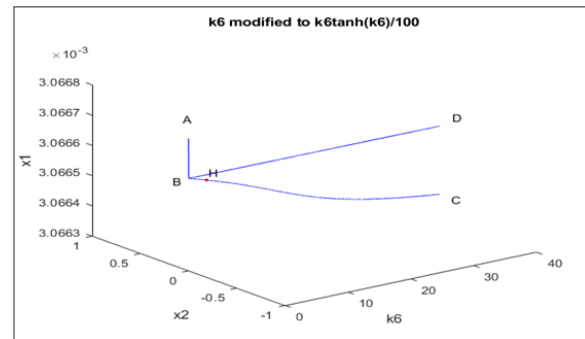


Figure 3: Bifurcation analysis with k_6 as bifurcation parameter.

When k_{11} was the bifurcation parameter, a Hopf bifurcation point was located at $(x_1, x_2, x_3, x_4, k_{11})$ values of $(0.003067, 0, 0, 0, 0, 0.062997)$ as shown in curve ABC in Fig. 4. When k_{11} was modified to $k_{11} \tanh(k_{11})/650$ the Hopf bifurcation disappears. This is shown in the curve ABD in Fig. 4.

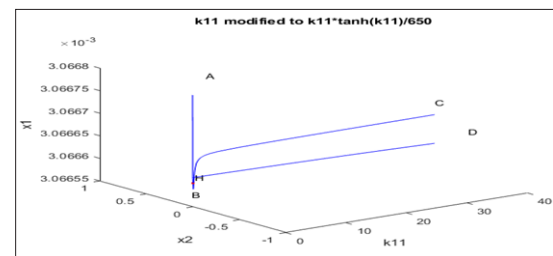


Figure 4: Bifurcation analysis with k_{11} as bifurcation parameter.

When k_{12} was the bifurcation parameter, two Hopf bifurcation points were located at $(x_1, x_2, x_3, x_4, k_{12})$ values of $(0.003067, 0, 0, 0, 0, 0.400456)$ and $(0.003067, 0, 0, 0, 0, 0.517213)$ as shown in curve ABC in Fig. 5. When k_{12} was modified to $k_{12} \tanh(k_{12})/0.005$ the Hopf bifurcation disappears. This is shown in the curve ADC in Fig. 5. With all the bifurcation parameters, the use of the tanh activation factor was successful in eliminating the Hopf bifurcation points that cause unwanted limit cycles and oscillatory behavior validating the analysis of Sridhar(2024)[38]

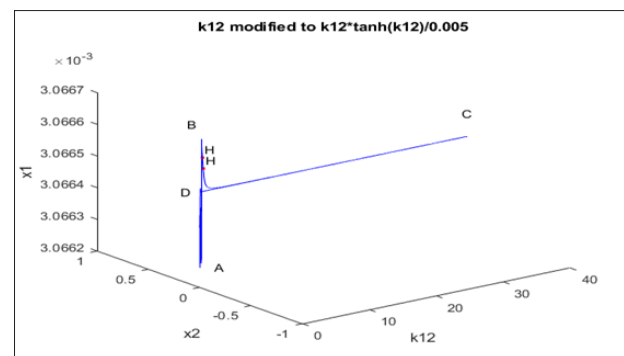


Figure 5: Bifurcation analysis with k_{12} as bifurcation parameter

For the MNLMPC calculations, $\sum_{t=0}^{t_f} x_1(t_i), \sum_{t=0}^{t_f} x_2(t_i), \sum_{t=0}^{t_f} x_3(t_i), \sum_{t=0}^{t_f} x_4(t_i), \sum_{t=0}^{t_f} x_5(t_i)$ were minimized individually and led to values of $0.135435E-02, 0, 0,$ and 0 . k_4 was the control parameter. The multiobjective optimal problem will involve the minimization of $(\sum_{t=0}^{t_f} x_1(t_i) - 0.135435E-02)^2 + (\sum_{t=0}^{t_f} x_2(t_i))^2 + (\sum_{t=0}^{t_f} x_3(t_i))^2 + (\sum_{t=0}^{t_f} x_4(t_i))^2 + (\sum_{t=0}^{t_f} x_5(t_i))^2$ subject to the equations governing the model. This led to a value of zero (the Utopia solution).

The control value k_4 stayed constant at 0.05. Figs 6, 7 and 8 show the various MNLMPC profiles.

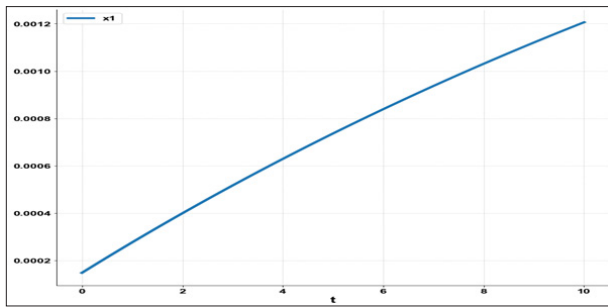


Figure 6: MNLMPC with x_1 vs t

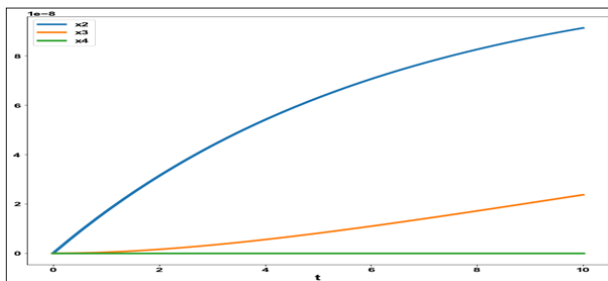


Figure 7: MNLMPC with x_2, x_3, x_4 vs t

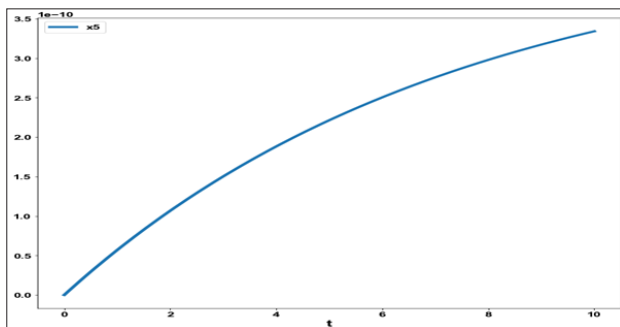


Figure 8: MNLMPC with x_5 vs t

Conclusions

Bifurcation analysis and multiobjective nonlinear model predictive control calculations were performed on a dynamic hypothalamic-pituitary-adrenal (HPA) axis model. The bifurcation analysis revealed the existence of a limit cycle causing Hopf bifurcation points, which are eliminated using an activation factor involving the tanh function. The multi-objective nonlinear model predictive calculations converged to the Utopia point (the best possible solution). The integration of the bifurcation analysis and multiobjective nonlinear model predictive control for a dynamic hypothalamic-pituitary-adrenal (HPA) axis model is the main contribution of this paper.

Data Availability Statement

All data used is presented in the paper

Conflict of interest

The author, Dr. Lakshmi N Sridhar has no conflict of interest.

Acknowledgement

Dr. Sridhar thanks Dr. Carlos Ramirez and Dr. Suleiman for encouraging him to write single-author papers.

References

1. Tsigos C, Chrousos GP (2002) "Hypothalamic-pituitary-adrenal axis, neuroendocrine factors and stress". *J Psychosom Res*, 53: pp865-871.
2. Savic D, Jelic S (2005) "A theoretical study of hypothalamo-pituitary adrenocortical axis dynamics". *Ann N Y Acad Sci*, 1048: pp 430-432.
3. Jelic S, Cupic , Kolarani_c Lj (2005) "Mathematical modeling of the hypothalamic-pituitary-adrenal system activity". *Math Biosci*, 197:pp173-187.
4. Lenbury Y, Pornsawad P (2005) "A delay-differential equation model of the feedback-controlled hypothalamus-pituitary-adrenal axis in humans". *Math Med Biol*, 22: pp15-33.
5. Kyrilov V, Severyanova LA, Vieira A (2005) "Modeling robust oscillatory behavior of the hypothalamic-pituitary-adrenal axis". *IEEE Trans Biomed Eng*, 52: pp1977-1983.
6. Savic D, Jeli_c S, Buri_c N (2006) "Stability of a general delay differential model of the hypothalamo-pituitary-adrenocortical system". *Int J Bifurc Chaos*, 16: pp3079-3085.
7. Smith SM, Vale WW (2006) "The role of the hypothalamic-pituitary-adrenal axis in neuroendocrine responses to stress". *Dialogues Clin Neurosci*, 8: pp383-395.
8. Gupta S, Aslakson E, et al; (2007) "Inclusion of the glucocorticoid receptor in a hypothalamic pituitary adrenal axis model reveals bistability". *Theor Biol Med Model*, 4: pp8.
9. Bairagi N, Chatterjee S, Chattopadhyay J (2008) "Variability in the secretion of corticotropin-releasing hormone, adrenocorticotrophic hormone and cortisol and understandability of the hypothalamic-pituitary-adrenal axis dynamics — a mathematical study based on clinical evidence". *Math Med Biol*, 25: pp37-63.
10. Vinther F, Andersen M, Ottesen JT (2011) "The minimal model of the hypothalamic-pituitary-adrenal axis". *J Math Biol*, 63: pp663-690.
11. Jelic S, Cupic , et al; (2011) "Predictive modeling of the hypothalamic-pituitary-adrenal (HPA) function. Dynamic systems theory approach by stoichiometric network analysis and quenching small amplitude oscillations". *Int J Nonlinear Sci Numer Simul*, 10: pp1451-1472.
12. Markovic VM, Cupi_c , et al; (2011) "Predictive modeling of the hypothalamic-pituitary-adrenal (HPA) axis response to acute and chronic stress". *Endocr J*, 58: pp889- 904.
13. Markovic VM, et al; (2011) "The stability of the extended model of hypothalamic-pituitary-adrenal axis examined by stoichiometric network analysis". *Russ J Phys Chem A*, 85: pp2327-2335.
14. Andersen M, Vinther F, et al; (2013) "Mathematical modeling of the hypothalamic-pituitary-adrenal gland (HPA) axis, including hippocampal mechanisms". *Math Biosci*, 246: pp122-138.

15. Postnova S, Fulcher R, et al; (2013) "A minimal physiologically based model of the HPA axis under influence of the sleep-wake cycles". *Pharmacopsychiatry*, 46(Suppl. 1):S36-S43.
16. Gudmand-Hoeyer J, et al; "Patient-specific modeling of the neuroendocrine HPA-axis and its relation to depression: ultradian and circadian oscillations". *Math Biosci*, 257: pp23-32.
17. Hosseinichimeh N, et al; (2015) "Modeling the hypothalamus-pituitary-adrenal axis: a review and extension". *Math Biosci*, 268: pp52-65
18. Malek H, et al; (2015) "Dynamics of the HPA axis and inflammatory cytokines: insights from mathematical modeling". *Comput Biol Med*, 67: pp1-12.
19. Markovic VM, et al; (2016) "Modelling cholesterol effects on the dynamics of the hypothalamic-pituitary-adrenal (HPA) axis". *Math Med Biol*, 33: pp1-28.
20. Cupic , Markovic VM, et al; (2016) "Dynamic transitions in a model of the hypothalamic-pituitary-adrenal axis". *Chaos*, 26: pp033111.
21. Pierre K, Schlesinger N, et al; (2016) "The role of the hypothalamic-pituitary-adrenal axis in modulating seasonal changes in immunity". *Physiol Genomics*, 48: pp719-738.
22. Abulseoud OA, et al (2017) "Corticosterone oscillations during mania induction in the lateral hypothalamic kindled rat-Experimental observations and mathematical modeling". *PLOS ONE*, 12: ppe0177551
23. Stanojevic A, et al; (2017) "Kinetic modelling of testosterone-related differences in the hypothalamic-pituitary-adrenal axis response to stress". *Reaction Kinetics, Mechanisms and Catalysis*.
24. Bangsgaard EO, Ottesen JT (2017) "Patient specific modeling of the HPA axis related to clinical diagnosis of depression". *Math Biosci*, 287: pp24-35.
25. Kim LU, D'Orsogna MR, Chou T et al; (2017) "Perturbing the hypothalamic-pituitary-adrenal stress response system: mathematical modeling to improve diagnosis of post-traumatic and related stress disorders". *Biophys J*, 112: pp284a.
26. Stanojevic A, et al; (2017) "Modelling of the hypothalamic-pituitary-adrenal axis perturbations by externally induced cholesterol pulses of finite duration and with asymmetrically distributed concentration profile". *Russ J Phys Chem A*, 91: pp112-119.
27. Kim LU, et al; (2017) "Perturbing the hypothalamic pituitary-adrenal axis: a mathematical model for interpreting PTSD assessment tests". *Comput Psychiatry*, 2: pp28-49.
28. Kaslik E, Neamtu M (2018) "Stability and Hopf bifurcation analysis for the hypothalamic-pituitary-adrenal axis model with memory". *Math Med Biol*, 35: pp49-78.
29. Dhooge A, et al; (2003) "A Matlab package for numerical bifurcation analysis of ODEs", *ACM transactions on Mathematical software* 29(2) pp.141-164.
30. Dhooge, A,W. Govaerts Y. et al; (2004), "CL_MATCONT"; *A continuation toolbox in Matlab*.
31. Kuznetsov Y.A. (1998) "Elements of applied bifurcation theory" .*Springer*,NY.
32. Kuznetsov,Y.A.(2009)."Five lectures on numerical bifurcation analysis" ,*Utrecht University,NL.*, 2009.
33. Govaerts, w. J. F, (2022) "Numerical Methods for Bifurcations of Dynamical Equilibria", *SIAM*, 2000.
34. Dubey S. R. Singh, S. K. & Chaudhuri B. B. (2022) "Activation functions in deep learning: A comprehensive survey and benchmark". *Neurocomputing*, 503, 92-108.
35. Kamalov A. F. Nazir M. Safaraliev A. K. Cherukuri and R. Zgheib 2021, "Comparative analysis of activation functions in neural networks," 28th IEEE International Conference on Electronics, Circuits, and Systems (ICECS), Dubai, United Arab Emirates, , pp. 1-6.
36. Szandała, T. (2020) "Review and Comparison of Commonly Used Activation Functions for Deep Neural Networks". *ArXiv*.
37. Sridhar. L. N. (2023)" Bifurcation Analysis and Optimal Control of the Tumor Macrophage Interactions". *Biomed J Sci & Tech Res* 53(5). BJSTR. MS.ID.008470.
38. Sridhar LN. (2024) "Elimination of oscillation causing Hopf bifurcations in engineering problems". *Journal of Applied Math*; 2(4): pp1826.
39. Flores-Tlacuahuac, A. et al; (2012) "Multiobjective Nonlinear model predictive control of a class of chemical reactors" . *I & EC research*; 5891-5899.
40. Hart William E, et al; "Pyomo – Optimization Modeling in Python" Second Edition. Vol. 67.
41. Wächter A, Biegler L. (2006) "On the implementation of an interior-point filter line-search algorithm for large-scale nonlinear programming". *Math. Program.* **106**, 25–57.
42. Tawarmalani, M. and N. V. Sahinidis, (2005) "A polyhedral branch-and-cut approach to global optimization", *Mathematical Programming*, 103(2), 225-249.